# Transport in Nanostructures and Nanotubes

Tsuneya Ando [1], Hidekatsu Suzuura

*Department of Physics, Tokyo Institute of Technology, 2-12-1 Ookayama, Meguro-ku, Tokyo 152-8551, Japan*

**Abstract**

In two-dimensional honeycomb lattices, electronic states are described by Weyl's equation for a massless neutrino when each site is occupied by an electron on average. The system has a topological singularity at the origin $\boldsymbol{k} = 0$ of the wave vector, giving rise to nontrivial Berry's phase when $\boldsymbol{k}$ is rotated around the origin. The singularity causes discrete jumps in the conductivity at the energy corresponding to $\boldsymbol{k} = 0$ in honeycomb lattices and leads to the absence of backscattering and a perfect conductance in carbon nanotubes.

*Key words:* honeycomb lattice; topological singularity; Berry's phase; anomaly

Since the discovery of carbon nanotubes [1], the transport property of the carbon network of the nanometer scale has attracted much attention. A carbon nanotube consists of coaxially rolled two-dimensional (2D) graphite sheets having a honeycomb lattice. A honeycomb lattice can be realized at semiconductor heterostructures with hexagonal antidot arrays. In this paper a review is given of effects a topological singularity present in the Schrödinger equation on transport properties of such honeycomb lattices and also of carbon nanotubes.

In a honeycomb lattice, a unit cell contains two carbon atoms denoted by A and B as shown in fig. 1. Two $\pi$ bands having approximately a linear dispersion cross the Fermi level at K and K' points of the first Brillouin zone. The effective-mass Hamiltonian for the K point in a magnetic field $B$ applied perpendicular to the system (the $xy$ plane) is given by

$$\gamma(\boldsymbol{\sigma}\cdot\hat{\boldsymbol{k}})\boldsymbol{F}(\boldsymbol{r}) = \varepsilon\boldsymbol{F}(\boldsymbol{r}), \quad \boldsymbol{F}(\boldsymbol{r}) = \begin{pmatrix} F_A(\boldsymbol{r}) \\ F_B(\boldsymbol{r}) \end{pmatrix}, \qquad (1)$$

where $\boldsymbol{\sigma} = (\sigma_x, \sigma_y)$ is the Pauli spin matrix, $\gamma$ is a band parameter, $\hat{\boldsymbol{k}} = -\mathrm{i}\boldsymbol{\nabla} + (e\boldsymbol{A}/c\hbar)$, with $\boldsymbol{A}$ the vector potential given by $\boldsymbol{B} = \mathrm{rot}\boldsymbol{A}$, and $F_A$ and $F_B$ represent the amplitude at two carbon sites A and B, respectively [2,3]. The above equation is same as Weyl's equation for a neutrino with vanishing rest mass and constant velocity independent of the wave vector.

It is known that a neutrino has a helicity and its spin is quantized into the direction of its motion. In fact, in the absence of a magnetic field, the eigen wavefunction and the corresponding energy bands are given by

$$\boldsymbol{F}_{s\boldsymbol{k}}(\boldsymbol{r}) = \frac{1}{\sqrt{2}L}\begin{pmatrix} \mathrm{e}^{\mathrm{i}\varphi(\boldsymbol{k})} \\ s \end{pmatrix}\exp(\mathrm{i}\boldsymbol{k}\cdot\boldsymbol{r}), \ \ \varepsilon_s(\boldsymbol{k}) = s\gamma k, \ (2)$$

where $L^2$ is the system area, $\varphi(\boldsymbol{k})$ is the angle of the wave vector $\boldsymbol{k} = (k_x, k_y)$, $k = |\boldsymbol{k}|$, and $s = +1$ and $-1$ for the conduction and valence bands, respectively. The velocity is given by $|\boldsymbol{v}| = \gamma/\hbar$ independent of $\boldsymbol{k}$ and $\varepsilon$. The density of states becomes $D(\varepsilon) = |\varepsilon|/2\pi\gamma^2$, which varies linearly as a function of the energy and vanishes at $\varepsilon = 0$. Figure 2 shows the energy dispersion and the density of states of the system described by eq. (1).

The above wave function acquires Berry's phase $-\pi$ when the wave vector $\boldsymbol{k}$ is rotated around the origin, although it looks continuous as a function of $\boldsymbol{k}$ [4,5]. This is equivalent to the well-known signature change of the spinor wave function or a spin rotation operator under a $2\pi$ rotation.

It should be noted that $\varphi = -\pi$ when the closed contour encircles the origin $\boldsymbol{k} = 0$ but $\varphi = 0$ when the contour does not contain $\boldsymbol{k} = 0$. Further, the wave

[1] Corresponding author. E-mail: ando@stat.phys.titech.ac.jp

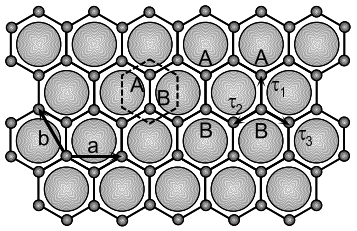


Fig. 1. The structure of a honeycomb lattice. A unit cell contains two atoms denoted as A and B (small circles). A honeycomb lattice can be realized at a semiconductor heterostructure by fabrication of a short-period hexagonal antidot array (shadowed big circles).

function at $\boldsymbol{k} = 0$ depends on the direction of $\boldsymbol{k}$ and its "spin" direction is undefined. These facts show the presence of a topological singularity at $\boldsymbol{k} = 0$. This topological singularity causes a zero-mode anomaly in the conductivity of the honeycomb lattice and also the absence of backscattering in metallic carbon nanotubes as will be demonstrated below.

A singularity at $\varepsilon = 0$ manifests itself in magnetic fields even in classical mechanics. The equation of motion gives the cyclotron frequency $\omega_c = eBv^2/c\varepsilon$, where $v$ is the electron velocity given by $v = |\boldsymbol{v}| = \gamma/\hbar$. The cyclotron frequency $\omega_c$ diverges and changes its signature at $\varepsilon = 0$ [6]. In quantum mechanics $\hat{k}_x$ and $\hat{k}_y$ satisfy the commutation relation $[\hat{k}_x, \hat{k}_y] = -\mathrm{i}/l^2$, where $l$ is the magnetic length given by $\sqrt{c\hbar/eB}$. Semiclassically, the Landau levels can be obtained as $\varepsilon_n = \pm\sqrt{n+\delta}\,(\sqrt{2}\gamma/l)$ with integer $n$ and an appropriate small correction $\delta$. Because of the uncertainty relation, $k^2 = 0$ is not allowed and there is no Landau level at $\varepsilon = 0$. However, a quantum mechanical treatment of a magnetic field leads immediately to the formation of Landau levels at $\varepsilon = 0$.

We consider, for example, a system with scatterers with a potential range much smaller than the typical electron wavelength (which is infinite at $\varepsilon = 0$) [7]. The relaxation time in the absence of a magnetic field becomes $\tau_0^{-1} = 2\pi|\varepsilon|W/\hbar$ with $W$ being a dimensionless parameter to characterize the scattering strength given by $W = n_i\langle(u_i)^2\rangle/4\pi\gamma^2$, where $u_i$ and $n_i$ are the strength and the concentration of scatterers, respectively, and $\langle\cdots\rangle$ means the average over impurities.

With the use of the Boltzmann transport equation, the transport relaxation time becomes $\tau(\varepsilon) = 2\tau_0(\varepsilon)$ and the conductivity $\sigma_0 = (e^2/2\pi^2\hbar)W^{-1}$ independent of the Fermi level, i.e., nonzero even at $\varepsilon = 0$ where the density of states vanishes.

In the presence of a magnetic field, the conductivity tensor $\sigma_{\mu\nu}$ with $\mu = x, y$ and $\nu = x, y$ is given by $\sigma_{xx} = \sigma_{yy} = \sigma_0/[1+(\omega_c\tau)^2]$ and $\sigma_{xy} = -\sigma_{yx} = -\sigma_0\omega_c\tau/[1+(\omega_c\tau)^2]$. Using the explicit expressions for $\omega_c$ and $\tau$, we have $\sigma_{xx} = \sigma_0\xi^4/(1+\xi^4)$ and $\sigma_{xy} = -\sigma_0\xi^2/(1+\xi^4)$, with $\xi = \sqrt{2\pi\alpha W}(\varepsilon_F/\varepsilon_B)$, where $\varepsilon_B$ is the magnetic

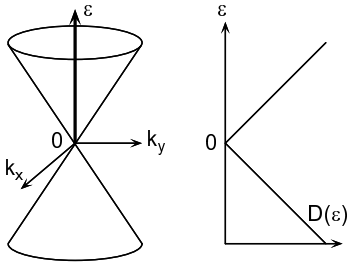


Fig. 2. The energy dispersion and density of states in the vicinity of the Fermi level in a honeycomb lattice.

energy defined by $\varepsilon_B = \gamma/l$. Because $\tau(\varepsilon_F)^{-1} \propto |\varepsilon_F|$, the dependence on the Fermi energy $\varepsilon_F$ is fully scaled by $\varepsilon_B$. Therefore, the conductivities exhibit a singular jump to zero at $\varepsilon_F = 0$ from $\sigma_0$ for nonzero $\varepsilon_F$ in the limit of the vanishing magnetic field $\varepsilon_B \to 0$.

A singular behavior appears also in the dynamical conductivity [8]. The dynamical conductivity is calculated as

$$\sigma(\omega) = \frac{e^2}{8\hbar}\Big[\frac{4}{\pi}\frac{\mathrm{i}\varepsilon_F}{\hbar\omega + \mathrm{i}[\hbar/\tau(\varepsilon_F)]} + 1 + \frac{\mathrm{i}}{\pi}\ln\frac{\hbar\omega + \mathrm{i}[\hbar/\tau(\hbar\omega/2)] - 2\varepsilon_F}{\hbar\omega + \mathrm{i}[\hbar/\tau(\hbar\omega/2)] + 2\varepsilon_F}\Big]. \tag{3}$$

Because $\hbar/\tau(\varepsilon) \propto |\varepsilon|$, the frequency dependence is scaled by $\hbar\omega/\varepsilon_F$. The scaling of the dynamical conductivity $\sigma(\hbar\omega/\varepsilon_F)$ shows that $\sigma(\omega, \varepsilon_F)$ exhibits a singular behavior at the point $(\omega, \varepsilon_F) = (0, 0)$. The correct way is to let $\omega \to 0$ at each $\varepsilon_F$, leading to a singular jump of the static conductivity to $e^2/8\hbar$ from $\sigma_0$ at $\varepsilon_F = 0$.

A more refined treatment in a self-consistent Born approximation (SCBA) has been performed for the magnetoconductivity in a self-consistent Born approximation in which level-broadening effects are properly taken into account [9]. The result shows that the conductivity at $\varepsilon_F = 0$ is given by $e^2/\pi^2\hbar$, which is universal and independent of the scattering strength. Figure 3 shows some examples of the calculated $\varepsilon_F$ dependence of $\sigma$. It varies smoothly across $\varepsilon_F = 0$ but exhibits a sharp jump in the limit of weak scattering ($W \ll 1$) from the Boltzmann result $\sigma_0$ for $\varepsilon \neq 0$ down to $\sigma = e^2/\pi^2\hbar$ at $\varepsilon_F = 0$.

A similar calculation was performed quite recently for the dynamical conductivity [8]. The frequency dependence is scaled by $\hbar\omega/\varepsilon_F$ as long as $\varepsilon_F \neq 0$. When $\varepsilon_F$ is very close to 0, however, the conductivity at $\omega = 0$ becomes small and the discrete jump present in the Boltzmann conductivity is removed. The energy scale causing this crossover behavior becomes smaller for smaller $W$ leading to a singular behavior of the dynamical conductivity in the weak scattering limit.

The electronic states of a carbon nanotube can be obtained by imposing periodic boundary conditions in

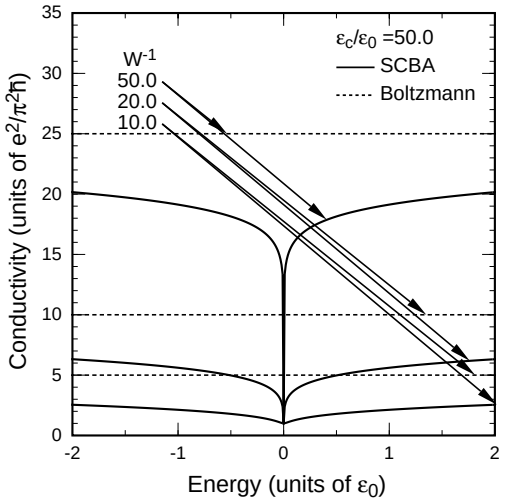


Fig. 3. An example of the conductivity vs the Fermi energy. The solid lines represent the conductivity calculated in SCBA and horizontal dotted lines the corresponding Boltzmann result. $\varepsilon_0$ is an arbitrary energy scale. After Ref. [9].

the circumference direction except in extremely thin tubes, i.e., $\psi(\boldsymbol{r}+\boldsymbol{L})=\psi(\boldsymbol{r})$, where $\boldsymbol{L}$ is called the chiral vector and corresponds to the circumference of a nanotube. The angle $\eta$ of $\boldsymbol{L}$ measured from the horizontal direction in fig. 1 is called the chiral angle. Carbon nanotubes can be either a metal or semiconductor, depending on their diameters and helical arrangement. These conditions were first predicted by means of a tight-binding model. They can be well reproduced in the $\boldsymbol{k}\cdot\boldsymbol{p}$ scheme discussed above [3].

In the $\boldsymbol{k}\cdot\boldsymbol{p}$ scheme, electrons in a nanotube can be regarded as neutrinos on a cylinder surface with a fictitious Aharonov-Bohm (AB) magnetic flux determined by $\boldsymbol{L}$. In metallic tubes, the flux vanishes and $\boldsymbol{F}$ satisfies periodic boundary conditions, while in semiconducting tubes, conditions for $\boldsymbol{F}$ include a nonzero AB phase. This $\boldsymbol{k}\cdot\boldsymbol{p}$ scheme has been used successfully in the study of wide varieties of electronic properties of CN. Some of such examples are magnetic properties [10] including the AB effect on the band gap, optical absorption spectra [11], exciton effects [12], lattice instabilities in the absence [13,14] and presence of a magnetic field [15], magnetic properties of ensembles of nanotubes [16], effects of spin-orbit interaction [17], junctions [18], topological defects [19], and electronic properties of nanotube caps [20].

The nontrivial Berry's phase leads to the unique property of a metallic carbon nanotube that there exists no backscattering and the tube is a perfect conductor even in the presence of scatterers [5,7]. In fact, it has been proved that the Born series for backscattering vanish identically [7]. Further, the conductance has been calculated exactly for finite-length nanotubes containing many impurities. The absence of backscattering has been confirmed also by numerical calculations in a tight binding model [21].

Backscattering corresponds to a rotation of the $\boldsymbol{k}$ direction by $\pm\pi$. In the absence of a magnetic field, there exists a time reversal process corresponding to each backscattering. This process corresponds to a rotation by $\pm\pi$ in the opposite direction. The scattering amplitude of these two processes is same in the absolute value but has an opposite signature because of Berry's phase. As a result, the backscattering amplitude cancels out completely. In semiconducting nanotubes, on the other hand, backscattering appears because the symmetry is destroyed by a nonzero AB magnetic flux.

An important information has been obtained on the effective mean free path in nanotubes by single-electron tunneling experiments [22,23]. The Coulomb oscillation in semiconducting nanotubes is quite irregular and can be explained only if nanotubes are divided into many separate spatial regions in contrast to that in metallic nanotubes [24]. This behavior is consistent with the presence of considerable amount of backward scattering leading to a strong localization of the wave function. In metallic nanotubes, the wave function is extended in the whole region of a nanotube because of the absence of backward scattering. With the use of electrostatic force microscopy the voltage drop in a metallic nanotube has been shown to be negligible in comparison with an applied voltage [25].

At nonzero temperatures, lattice vibrations usually constitute the major source of electron scattering and limit the resistivity. Usually long-wavelength acoustic phonons are most important. These modes can be described by a continuum model [26–28]. An acoustic phonon gives rise to an effective electron-phonon coupling called the deformation potential $V_1=g_1(u_{xx}+u_{yy})$ with $u_{xx}=(\partial u_x/\partial x)+(u_z/R)$ and $u_{yy}=\partial u_y/\partial y$, where $u_x$, $u_y$, and $u_z$ represent lattice displacements in the $x$, $y$, and $z$ directions, respectively. This potential appears as a diagonal term. A very rough estimation gives $g_1\sim 30$ eV.

Phonon cause also a change in the distance between neighboring carbon atoms. This gives rise to an off-diagonal elements $V_2=g_2\mathrm{e}^{3\mathrm{i}\eta}(u_{xx}-u_{yy}+2\mathrm{i}u_{xy})$ with $g_2=(3\alpha\beta/4)\gamma_0$, where $-\gamma_0$ is the transfer between nearest-neighbors, $\beta=-\mathrm{d}\ln\gamma_0/\mathrm{d}\ln b$, $b$ is the bond length, and $\alpha$ is a quantity smaller than unity dependent on microscopic models of phonons. Usually, we have $\beta\sim 2$ [29] and $\alpha\sim 1/3$, which give $g_2\sim\gamma_0/2$ or $g_2\sim$ 1.5 eV. This coupling constant is much smaller than the deformation potential. It corresponds to one given by Kane and Mele [30] without the reduction factor $\alpha$.

The diagonal term does not contribute to the backscattering as in the case of impurities and only the much smaller off-diagonal term has some contribution. The mean free path $\Lambda$ is estimated as $\Lambda=$

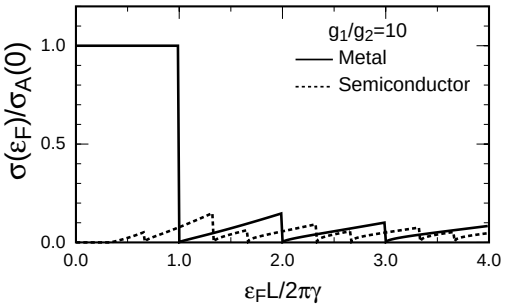


Fig. 4. The Fermi-energy dependence of the conductivity for metallic (solid line) and semiconducting (broken line) CN's with $g_1/g_2 = 10$ in units of $\sigma_A(0)$ denoting the conductivity of an armchair CN with $\varepsilon_F = 0$. After Ref. [28].

$(\mu a^2/3k_BT\alpha^2\beta^2)L$, where $L = |\boldsymbol{L}|$, $\mu$ is the shear modulus of 2D graphite, and $a$ is the lattice constant. We obtain $\Lambda \sim 600L$ at room temperature, which is larger than 1 $\mu$m for thin armchair nanotubes with diameter $\sim$1.5 nm and increases in proportion to $L$ with $L$. This shows that a metallic CN is ballistic even at room temperature. The situation changes dramatically when other bands start to be occupied. Figure 4 shows the Fermi energy dependence of the conductivity obtained by solving Boltzmann equation [28].

In summary, in two-dimensional honeycomb lattices the topological singularity present at $\boldsymbol{k} = 0$ gives rise to nontrivial Berry's phase of the wave function when the $\boldsymbol{k}$ is rotated around the origin. This singularity gives rise to discrete jumps in the Boltzmann conductivity at the energy corresponding to $\boldsymbol{k} = 0$. This jump is somewhat smoothed out but prevails practically even if level broadening effects are properly taken into account in the self-consistent Born approximation. In carbon nanotubes, this topological singularity leads to the absence of backscattering and a perfect conductance even in the presence of scatterers. Phonons cause backscattering at high temperatures, but effects are very weak and nanotubes are considered as ballistic conductors even at room temperature, because the strong deformation potential has no contribution.

## Acknowledgements

This work has been supported in part by Grants-in-Aid for COE (12CE2004 "Control of Electrons by Quantum Dot Structures and Its Application to Advanced Electronics") and Scientific Research from the Ministry of Education, Science and Culture, Japan.

## References

[1] S. Iijima, Nature (London) **354** (1991) 56.

[2] J. C. Slonczewski and P. R. Weiss, Phys. Rev. **109** (1958) 272.

[3] H. Ajiki and T. Ando, J. Phys. Soc. Jpn. **62** (1993) 1255.

[4] M. V. Berry, Proc. Roy. Soc. London **A392** (1984) 45.

[5] T. Ando, T. Nakanishi, and R. Saito, J. Phys. Soc. Jpn. **67** (1998) 2857.

[6] Y. Zheng and T. Ando. Phys. Rev. B (in press).

[7] T. Ando and T. Nakanishi, J. Phys. Soc. Jpn. **67** (1998) 1704.

[8] T. Ando, Y. Zheng, and H. Suzuura, J. Phys. Soc. Jpn. **71** (2002) 1318.

[9] N. H. Shon and T. Ando, J. Phys. Soc. Jpn. **67** (1998) 2421.

[10] H. Ajiki and T. Ando, J. Phys. Soc. Jpn. **62** (1993) 2470 [Errata, J. Phys. Soc. Jpn. **63** (1994) 4267].

[11] H. Ajiki and T. Ando, Physica B **201** (1994) 349; Jpn. J. Appl. Phys. Suppl. **34-1** (1995) 107.

[12] T. Ando, J. Phys. Soc. Jpn. **66** (1997) 1066.

[13] N. A. Viet, H. Ajiki, and T. Ando, J. Phys. Soc. Jpn. **63** (1994) 3036.

[14] H. Suzuura and T. Ando, *Proceedings of 25th International Conference on the Physics of Semiconductors*, edited by N. Miura and T. Ando (Springer, Berlin, 2001), p. 1525.

[15] H. Ajiki and T. Ando, J. Phys. Soc. Jpn. **64** (1995) 260; **65** (1996) 2976.

[16] H. Ajiki and T. Ando, J. Phys. Soc. Jpn. **64** (1995) 4382.

[17] T. Ando, J. Phys. Soc. Jpn. **69** (2000) 1757.

[18] H. Matsumura and T. Ando, J. Phys. Soc. Jpn. **67** (1998) 3542; **70** (2001) 2401; Mol. Crys. Liq. Crys. **340** (2000) 725; *Proceedings of 25th International Conference on the Physics of Semiconductors*, edited by N. Miura and T. Ando (Springer, Berlin, 2001), p. 1655.

[19] H. Matsumura and T. Ando, J. Phys. Soc. Jpn. **70** (2001) 2657.

[20] T. Yaguchi and T. Ando, J. Phys. Soc. Jpn. **70** (2001) 3641; J. Phys. Soc. Jpn. (submitted for publication)

[21] T. Nakanishi and T. Ando, J. Phys. Soc. Jpn. **68** (1999) 561.

[22] S. J. Tans, M. H. Devoret, H. Dai, A. Thess, R. E. Smalley, L. J. Geerligs, and C. Dekker, Nature (London) **386** (1997) 474.

[23] A. Bezryadin, A. R. M. Verschueren, S. J. Tans, and C. Dekker, Phys. Rev. Lett. **80** (1998) 4036.

[24] P. L. McEuen, M. Bockrath, D. H. Cobden, Y. -G. Yoon, and S. G. Louie, Phys. Rev. Lett. **83** (1999) 5098.

[25] A. Bachtold, M. S. Fuhrer, S. Plyasunov, M. Forero, E. H. Anderson, A. Zettl, and P. L. McEuen, Phys. Rev. Lett. **84** (2000) 6082.

[26] H. Suzuura and T. Ando, Physica E **6** (2000) 864.

[27] H. Suzuura and T. Ando, Mol. Cryst. and Liq. Cryst. **340** (2000) 731.

[28] H. Suzuura and T. Ando, Phys. Rev. B **65** (2002) 235412.

[29] See for example, W. A. Harrison, *Electronic Structure and the Properties of Solids* (W.H. Freeman and Company, San Francisco, 1980).

[30] C. L. Kane and E. J. Mele, Phys. Rev. Lett. **78** (1987) 1932.